

Advanced Car Driving Assistant System: A Deep Non-local Pipeline Combined with 1D Dilated CNN for Safety Driving

Francesco Rundo¹, Roberto Leotta², Francesca Trenta², Giovanni Bellitto³,
Federica Proietto Salanitri³, Vincenzo Piuri⁴, Angelo Genovese⁴, Ruggero Donida Labati⁴,
Fabio Scotti⁴, Concetto Spampinato³ and Sebastiano Battiato²

¹STMicroelectronics, ADG Central R&D, Italy

²University of Catania, IPLAB Group, Italy

³University of Catania, PerCeive Lab, Italy

⁴University of Milan, Computer Science Department, Italy

Keywords: Drowsiness, Deep Learning, D-CNN, Deep-LSTM, PPG (PhotoPlethysmoGraphy).

Abstract: Visual saliency refers to the part of the visual scene in which the subject's gaze is focused, allowing significant applications in various fields including automotive. Indeed, the car driver decides to focus on specific objects rather than others by deterministic brain-driven saliency mechanisms inherent perceptual activity. In the automotive industry, vision saliency estimation is one of the most common technologies in Advanced Driver Assistant Systems (ADAS). In this work, we proposed an intelligent system consisting of: (1) an ad-hoc Non-Local Semantic Segmentation Deep Network to process the frames captured by automotive-grade camera device placed outside the car, (2) an innovative bio-sensor to perform car driver PhotoPlethysmoGraphy (PPG) signal sampling for monitoring related drowsiness and, (3) ad-hoc designed 1D Temporal Deep Convolutional Network designed to classify the so collected PPG time-series providing an assessment of the driver attention level. A downstream check-block verifies if the car driver attention level is adequate for the saliency-based scene classification. Our approach is extensively evaluated on DHIFK dataset, and experimental results show the effectiveness of the proposed pipeline.

1 INTRODUCTION

The term "drowsiness" indicates a state characterized by a low level of awareness and difficulty in maintaining the wakeful state. Driver's drowsiness may cause serious road traffic accidents involving vehicles. In the automotive field, the ability of detecting an attention state of a driver may facilitate evaluation of his/her fitness to drive a vehicle, preventing road accidents. In this respect, several studies have highlighted the correlation between the level of attention and Heart Rate Variability (HRV) of a subject (Igasaki et al., 2015). HRV is a measure of heart activity over beat-to-beat interval. Indeed, estimating HRV of a driver may permit to obtain useful information concerning possible drowsiness (Igasaki et al., 2015). Specifically, HRV reflects the heartbeat-to-beat interval that results mainly from the dynamic interaction between the Autonomous Nervous System and the heart (Igasaki et al., 2015; Cai et al., 2017; Winterlich et al., 2013). However, the driver's atten-

tion level must be adequate for the driving scenario. For instance, driving with low traffic and low speed requires a lower level of attention than a driving scenario that includes risky maneuvers (overtaking, lane changes, etc.) and at high speeds. Within this perspective, we propose an algorithm based on saliency analysis to understand the driving scenario in order to adjust the monitoring of the attention level accordingly. Saliency Detection is a method to identify the most outstanding and informative parts in a video or still image. It has been widely studied in such different kind of applications including automotive (Cai et al., 2017; Winterlich et al., 2013). The proposed work will show how the saliency analysis is able to improve the robustness of the implemented car driver drowsiness pipeline. The paper is organized as follows. Section 2 reports a brief introduction on the related works. In Section 3, we provide details about the used hardware framework to acquire the PPG signal along with the related processing pipeline. In Section 4, we described our innovative Deep learning pipeline

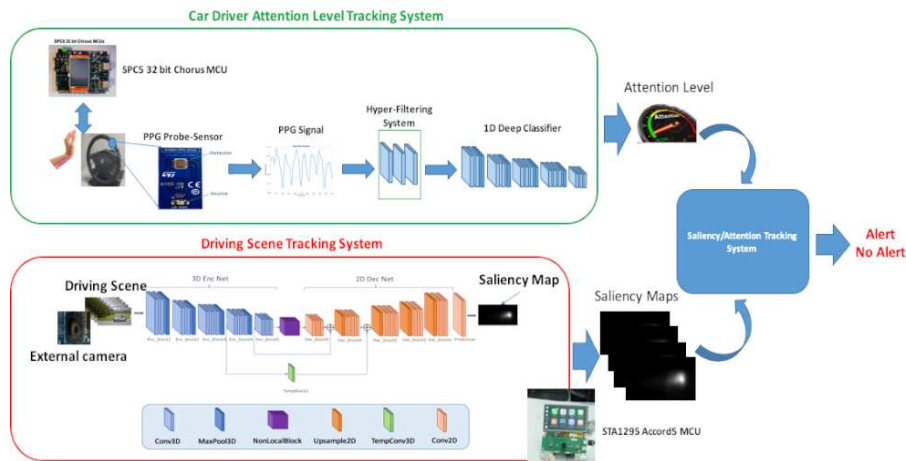


Figure 1: The overall scheme of the proposed pipeline.

to evaluate the car driver’s drowsiness alongside the driving scenario. Finally, experimental results and future works are reported in Section 5.

2 RELATED WORKS

In this section, we summarize previous approaches on evaluating car-driver attention level as well as driving scene understanding. In (Vicente et al., 2011), the authors introduced an innovative pipeline for monitoring a car driver’s drowsiness analyzing the ElectroCardio-Graphy (ECG) signal alterations analysis, which may introduce noise and artifacts while measuring HRV. Indeed, they proposed a pipeline to perform ECG signal stabilization and classification based on classical linear discriminant analysis. In (Szypulska and Piotrowski, 2012), the authors proposed a reliable approach for detecting fatigue and sleep onset. Specifically, the authors showed a method to discriminate activity, drowsiness, and sleep, taking into account the LF/HF ratio detected over the R-R tachogram computed from the ECG frequency analysis. The results obtained are promising and can be used to develop a drowsiness detection system for ADAS applications. In (Fujiwara et al., 2018), the authors analyzed specific changes in sleep condition by using the HRV signal. The authors proposed eight hand-crafted HRV signal features to be processed using a multivariate statistical process framework for detecting specific HRV dynamics. The results showed the effectiveness of the proposed method through standard confirmation based on usage of the ElectroEncephaloGraphy signal (EEG). Generally, existing approaches based on HRV detection propose invasive ECG sampling. In particular, it is necessary to have

at least three electrodes in contact with the human skin according to the minimum configuration known as Einthoven’s Triangle (Abi-Saleh and Omar, 2019). Both car driver’s hands must remain on the steering wheel where the two electrodes of the ECG signal sampling system are usually placed. Then, the third electrode is placed on the driver’s seat. This requirement raises a specific well-known issue related to the robustness of the ECG signal sampling system in automotive applications (Abi-Saleh and Omar, 2019). For this reason, many authors have proposed methods based on the PhotoPlethysmography (PPG) signal analysis rather than on the ECG. In (Rundo et al., 2018b), the authors presented a solution for evaluating the HRV from the PPG signal to analyze parasympathetic nervous activity and classify the subject’s drowsiness level. The obtained results confirmed the robustness of the proposed approach based on applying a low-power PPG probe. In (Rundo et al., 2018b; Rundo et al., 2018c), the authors proposed an interesting indicator from the PPG signal, which has been analyzed. In (Xu et al., 2012; Kurian et al., 2014), the authors implemented effective algorithms based on PRV (Pulse Rate Variability) data processing as a measure of the ANS and then the drowsiness of the subject. An interesting approach has been proposed in (Ryu et al., 2018) in which the authors projected a flexible sensor array composed of red organic light-emitting diodes (OLEDs) and organic photodiodes (OPDs) for detection of photoplethysmographic (PPG) signal. The reported test benchmarks in (Ryu et al., 2018) confirmed that the proposed flexible PPG sensor estimates the drowsiness with high accuracy concerning the classical PPG probe. Over the last years, researchers have investigated the use of Deep Learning in order to estimate the drowsiness of a subject from bio-signals and imaging. In (Hong and

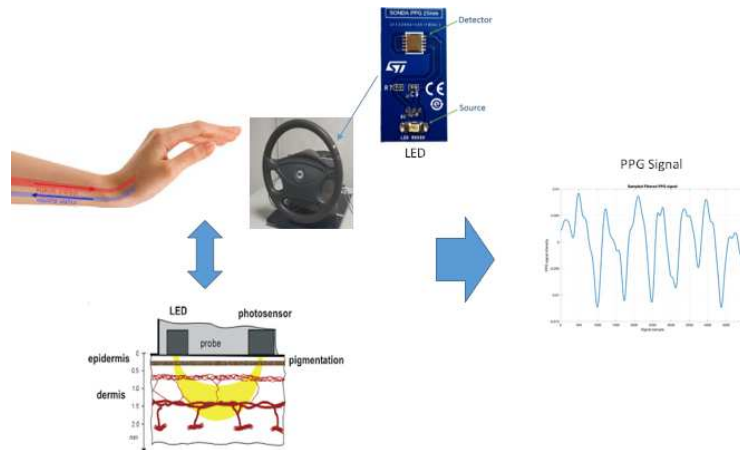


Figure 2: The PPG pattern formation scheme.

Qin, 2007; Alshaqqaqi et al., 2013), the authors proposed effective pipelines in order to estimate the car-driver drowsiness by examining the "eye state" of the driver through applying such image processing methods. However, the main issues of the proposed solutions involve the quality of video frames. Indeed, the effectiveness of these approaches may be affected by environmental conditions (illumination, occlusions, etc.) of the passenger compartment. As introduced, recent Deep learning advances in automotive applications allow such innovation in the field of the Drowsiness Detection system as confirmed by the pipeline proposed in (Sari and Huang, 2016). In (Sari and Huang, 2016), the authors presented an intelligent algorithm consisting of the wavelet packet transform (WPT) and a functional-link-based fuzzy neural network (FLFNN) to provide early detection of car-driver drowsiness. The drowsiness analysis is based on the HF/LF analysis (Alshaqqaqi et al., 2013). A similar approach was proposed in (Cheon and Kang, 2017), where a Support Vector Machine (SVM) approach has been successfully applied to classify the car-driver physiological data coming from an array of bio-sensors placed over the steering wheel. Another promising approach is (Choi et al., 2018) in which the authors designed a system based on Multimodal Deep Learning that recognizes both visual and physiological changes in the state of attention of the driver. More specifically, they used a deep learning framework consisting of Long Short-Term Memory (LSTM) to classify the driver's condition based on both visual and physiological data properly pre-processed. The results reported in (Choi et al., 2018) confirmed the robustness of the proposed approach. In (Altun and Celenk, 2017), the authors introduced an interesting vision-based driver assistance system for scene awareness using video saliency analysis.

The results reported that the proposed pipeline was able to detect how the driver's gaze was focused during driving. In (Deng et al., 2016), the authors collected the eye-tracking data of 40 subjects consisting of non-drivers and experienced drivers when viewing 100 traffic images. In particular, the authors proposed a solution to assess the drowsiness level and a monitoring system regulated by the information of the driving scenario.

3 METHODS AND MATERIALS

This section describes the overall pipeline. The attention level tracking system is described first. Afterwards, we introduced a Visual Saliency Scene pipeline. Finally, we provide details about our implemented ad-hoc Saliency/Attention Tracking System to evaluate the driver's attention level determined by the analysis of the car driver PPG signal with the saliency map. The Fig. 1 shows the overall scheme of the proposed pipeline. The following sections describe each of the blocks included in the pipeline shown in Fig. 1.

3.1 The Car Driver Attention Level Tracking System

This system is based on the usage of PPG signal sampled from the car driver to track the corresponding attention level. We provide hereinafter a brief introduction to PPG signal. The PPG sampling is a non-invasive method to monitor cardiovascular dynamic of a subject. Both heart health as well as respiratory rate and vascular disorders may be monitored by means of ad-hoc analysis of such PPG signal dynamic

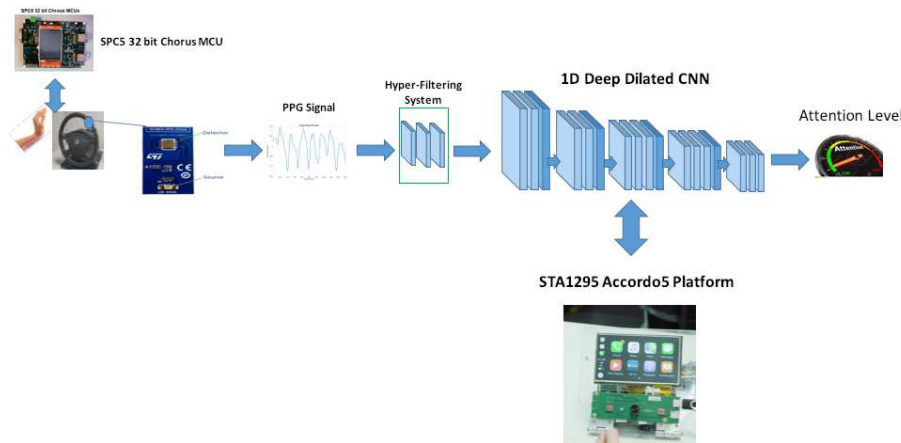


Figure 3: The proposed driver drowsiness monitoring pipeline.

(Rundo et al., 2018b). In few words, by means of ad-hoc analysis of the PPG signal we are able to collect a non-invasive measure of the heart activity and blood volume dynamic. A classical PPG raw waveform is composed by a pulsatile ('AC') physiological signal which is correlated to cardiac-synchronous changes in the blood volume (in sync with heart-beat) superimposed with a slowly varying ('DC') component containing lower frequency signals which is correlated to respiration, thermoregulation and skin tissues (in which the PPG sensor is plugged). For each cardiac cycle the heart pumps blood to the subject body with a specific pressure enough to distend the arteries and arterioles in the subcutaneous tissue. Through a simple sensing device composed by a light-emitter and a photo-detector attached over the subject skin, the blood volume changes can be detected as part of the PPG dynamic. More in details, the change in volume caused by the heart pressure pulse can be detected by illuminating the skin and then by measuring the amount of back-scattered light either transmitted or reflected to the photo-detector (Rundo et al., 2018b). Further information about PPG pattern formation and dynamics are provided in (Rundo et al., 2018b). The Fig. 2 shows the physiological phenomena underlying PPG waveform(s) formation as previously described. For the proposed pipeline, the authors implemented a PPG sensing device composed by a Silicon Photomultiplier sensor coupled with a LEDs emitter (Vinciguerra et al., 2018; Mazzillo et al., 2018; Rundo et al., 2019a; Rundo et al., 2019b).

The proposed PPG sensing probe is composed by a large area n-on-p Silicon Photomultipliers (SiPMs) fabricated at STMicroelectronics (Mazzillo et al., 2018). The used SiPMs array device has a total area of $4.0 \times 4.5 \text{ mm}^2$ and 4871 square microcells with $60 \mu\text{m}$ pitch. The devices have a geometrical fill factor of

67.4% and are packaged in a surface mount housing (SMD) with about $5.1 \times 5.1 \text{ mm}^2$ total area (Fujiwara et al., 2018). We used a Pixelteq dichroic bandpass filter with a pass band centered at about 540 nm with a Full Width at Half Maximum (FWHM) of 70 nm and an optical transmission higher than 90 – 95% in the pass band range was glued on the SMD package by using a Loctite 352TM adhesive. With the dichroic filter at 3V-OV the SiPM has a maximum detection efficiency of about 30% at 565 nm and a PDE of about 27.5% at 540 nm (central wavelength in the filter pass band). From our studies we obtained that the so implemented dichroic filter reduces the absorption of environmental light of more than 60% when the detector works in the linear range in Geiger mode above its breakdown voltage ($\sim 27 \text{ V}$). As described, the PPG detector needs a light emitter together with the introduced detector based on SiPM technology. We have used successfully the OSRAM LT M673 LEDs in SMD package emitting at 529 nm and based on In-GaN technology (Fujiwara et al., 2018). The used LEDs devices have an area of $2.3 \times 1.5 \text{ mm}^2$, viewing angle of 120° , spectral bandwidth of 33 nm and lower power emission (mW) in the standard operation range. The authors to get the PPG probe easily to use, have designed a printed circuit board (PCB) handled by a user-interface developed over the NI (National Instruments) equipment. The PCB is populated by a 4 V portable battery, a power management circuits, a conditioning circuit for output SiPMs signals, several USB connectors for PPG probes and related SMA output connectors. About the used hardware, more implementation details can be found in (Vinciguerra et al., 2018; Mazzillo et al., 2018; Rundo et al., 2019a; Rundo et al., 2019b). An implemented set of PPG sensing probes have been placed in the steering of the car where statistically it is more likely

Table 1: Hyper low-pass filtering setup (in Hz).

F	f1	f2	f3	f4	f5	f6	f7	f8	f9	f10	f11
HP	0.5	/	/	/	/	/	/	/	/	/	/
LP	0	1.5	2.2	2.3	3.1	3.9	4.2	4.3	5	5.9	6.9

Table 2: Hyper high-pass filtering setup (in Hz).

F	f1	f2	f3	f4	f5	f6	f7	f8	f9	f10	f11
HP	0.5	1.2	3	3.2	3.3	3.9	4.2	4.5	5	5.7	6.9
LP	7	/	/	/	/	/	/	/	/	/	/

that the driver rests his hand. Please note that to sample the PPG signal a single driver’s hand only (placed on top of the embedded PPG sensor probe) is needed in order to trigger the detecting of the physiological signal. In this way we have covered the first issue aforementioned and related to the use of the ECG difficult to be sampled on the car. As showed in Fig. 2, the proposed PPG sensing probe is embedded in the car steering. We populated the car steering with different PPG sending devices. More details about the hardware setup of this solution can be found (Vinciguerra et al., 2018; Mazzillo et al., 2018; Rundo et al., 2019a). The sampled PPG raw data will be fed into SP5C Chorus Dual Cortex A7 Microcontrollers (MCUs) having ad-hocs Analog to Digital Converters (ADCs) ports. An overall scheme of the proposed PPG based pipeline is reported Fig. 3 (Rundo et al., 2019b).

In the following paragraphs the pipeline reported in Fig. 3 will be detailed. Preliminary, we confirmed that the PPG waveforms (raw data) of the car driver will be collected as per scheme reported in Fig. 1. The sampled raw PPG signal will be furtherly processed by the hyper-filtering system (Rundo et al., 2019b) having the cut-off frequencies reported in Tables 1, 2. The collected hyper-filtered PPG signal patterns (Mazzillo et al., 2018) were classified by ad-hoc designed 1D Temporal Dilated Convolutional Neural Network as reported in Fig. 3. The main building block consists of a dilated causal convolution layer that operates over the time steps of each sequence. The proposed 1D-CNN includes multiple residual blocks, each containing two sets of dilated causal convolution layers with the same dilation factor, followed by normalization, ReLU activation, and spatial dropout layers. Furthermore, a $1 - by - 1$ convolution is applied to adapt the number of channels between the input and output as well as a final activation function. Specifically, we implemented a 1D pipeline composed of 18 blocks with a downstream softmax layer. Each of the Deep blocks comprises a dilated convolution layer with 3×3 kernel filters, a spatial dropout layer, another dilated

convolution layer, a ReLU layer, and a final spatial dropout. The dilation size starts at two and increases for each block. A softmax layer completes the proposed pipeline. The so-designed 1D Dilated Temporal CNN output represents the drowsiness level of the car-driver from which the pipeline has sampled and processed the PPG signal. This output is a scalar number in the range $[0, 1]$ that defines the attention level of the car driver, i.e., from the drowsy driver (0) to wakeful driver (1). The obtained results confirmed that the proposed Deep Learning framework correctly estimates the driver’s drowsiness with high accuracy. The implemented 1D Deep CNN backbone is ported over the STA1295 Accord5 embedded MCU platform (Mazzillo et al., 2018).

3.2 The Video Saliency Scene Understanding Block

This block is able to generate the saliency map of the video frames representing the driving scene captured by the external automotive grade camera. The Fig. 4 shows the overall scheme of this block. The video frames acquired by the external camera device during the driving are processed by the implemented Non-Local Semantic Segmentation Fully Convolutional Network (NL-FCN) as schematized in Fig. 4. Semantic segmentation of the samples driving scene will be performed by the encoder/decoder architecture, which provides a saliency map representing the most salient object in the acquired video frames. The proposed NL-FCN architectures are composed of an encoder and a decoder block. The encoder block (3D Enc Net) performs spatiotemporal feature extraction, and it is composed of five blocks. The first two blocks are composed of two separable convolution layers with a $3 \times 3 \times 2$ kernel filter followed by batch normalization, ReLU layer, and a downstream $1 \times 2 \times 2$ max-pooling layer. The remaining three blocks consist of two separable convolution layers with a $3 \times 3 \times 3$ kernel filter followed by batch normalization, another convolutional layer with $3 \times 3 \times 3$ kernel, batch normalization, and ReLU with a down-

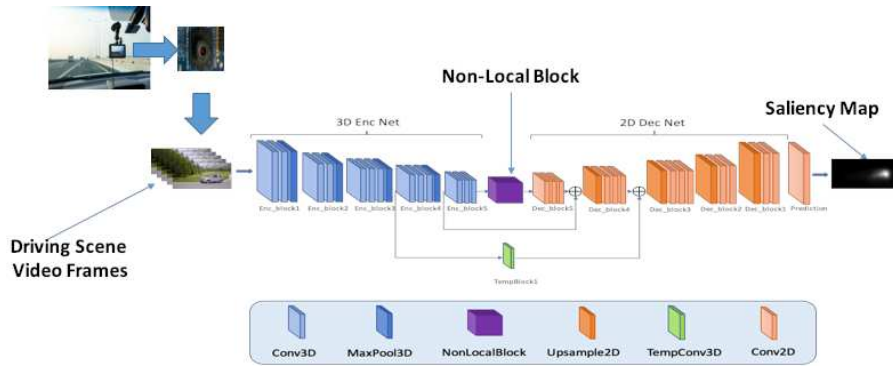


Figure 4: The proposed video saliency scene understanding block.

stream $1 \times 2 \times 2$ max-pooling layer. Furthermore, we inserted a Non-Local processing layer. Non-local blocks have been recently introduced (Wang et al., 2018) as a reliable approach for capturing space-time long-range dependencies and correlation on feature maps, providing a sort of “self-attention” mechanism. Self-attention through non-local blocks aims to enforce the model to extract correlation among feature maps by weighting the averaged features at all possible positions in the generated feature maps (Wang et al., 2018). In our pipeline, non-local block is able to extract features in dependencies at multiple abstract levels for holistic morphological modeling of the input driving scene frames. The mathematical formulation of non-local operation is reported in the following equations. Let x a general input data; the employed non-local operation computes the corresponding response y_i (of the given Deep architecture) at i location in the input data as a weighted sum of the input data at all positions $j \neq i$:

$$y_i = \frac{1}{\psi(x)} \sum_{\forall j} \zeta(x_i, x_j) \beta(x_j) \quad (1)$$

With $\zeta(\cdot)$ being a pairwise potential describing the affinity or relationship between data positions at index i and j respectively. $\beta(\cdot)$ is, instead, a unary potential modulating ζ according to input data. The sum is then normalized by a factor $\psi(x)$. The parameters of ζ , β and ψ potentials are learned during model’s training and defined as follows:

$$\zeta(x_i, x_j) = e^{\Theta(x_i)^T \Phi(x_j)} \quad (2)$$

Where Θ and Φ are two linear transformations of the input data x with learnable weights W_Θ and W_Φ :

$$\begin{aligned} \Theta(x_i) &= W_\Theta x_i \\ \Phi(x_j) &= W_\Phi x_j \\ \beta(x_j) &= W_\beta x_j \end{aligned} \quad (3)$$

For the $\beta(\cdot)$ function, a common linear embedding (classical $1 \times 1 \times 1$ convolution) with learnable weights W_β is employed. The normalization function ψ is:

$$\psi(x) = \sum_{\forall j} \zeta(x_i, x_j) \quad (4)$$

In Eqs. (1) - (4), and Embedded Gaussian setup is reported (Wang et al., 2018). The selection of the Embedded Gaussian based affinity function is compliant with recent self-attention approaches (Wang et al., 2018) specifically recommended for 2D or 3D applications. Through Non-Local Blocks, we capture long-range Spatio-temporal dependencies on the frames representing the driving scene, improving the capability of the saliency-based semantic segmentation pipeline. The Decoder backbone (2D Dec Net) decodes the visual features of the encoder. The Decoder Backbone shows a structure similar to the encoder one. Indeed, it comprises five blocks including 2D separable convolutional layers with 3×3 kernel, batch normalization layers, and ReLU. Such residual connections through a convolutional block are added. In particular, we have interpolated an up-sampling block (with a bi-cubic algorithm) to adjust the size of the feature maps. The output of the so-designed NL-FCN is the feature map of the acquired scene frame i.e., the segmented area of the most salient object. The Fig. 5 shows some instances of the saliency analysis of the video reporting the driving scene. In Fig. 5, some frames of a driving scenario are reported. The fixation point over the driving scene video frames represents the most salient area detected by our proposed NL-FCN architecture. The corresponding saliency map (output of the NL-FCN) is reported in Fig. 5. The NL-FCN has been trained and tested on the DHF1K dataset (Min and Corso, 2019). The proposed architecture reports acceptable performance on DHF1K dataset (Min and Corso, 2019) (Area Under the Curve: 0.875; Sim-



Figure 5: Saliency analysis of the video representing the driving scene.

ilarity: 0.318; Correlation Coefficient: 0.416; Normalized Scanpath Saliency: 2.613) compared with the performance of similar architectures (Min and Corso, 2019). However, we noticed that the architectures performing better than our pipeline are particularly complex computationally and require an expensive hardware. Conversely, our solution does not require specific hardware accelerations as it runs on the CPU in the STA1295 Accordo5 MCU platform (STMicroelectronics, 2019).

3.3 The Saliency/Attention Tracking System

This block is designed to evaluate the driver’s attention level determined by the PPG signal analysis with the saliency map generated by the NL-FCN block. Therefore, with a static saliency maps (low dynamic of the driving scene frames), the level of attention required does not necessarily have to be high. On the contrary, with a high temporal dynamic of the driving scene saliency map, the system checks if the car driver attention level is adequately high. Formally, if we set $S_f(x, y, t)$ as the saliency map and $O_c(t)$ the output of the 1D-CNN model, this block performs the following mathematical analysis:

$$V(S(x, y, t)) = \begin{cases} \frac{\partial S_f(x, y, t)}{\partial t} \leq \vartheta O_c(t) \leq \varphi \\ \frac{\partial S_f(x, y, t)}{\partial t} > \vartheta O_c(t) > \varphi \end{cases} \quad (5)$$

Basically, as described in Eq. 5 the Driver Attention Block checks the changing dynamic of the saliency map $S_f(x, y, t)$ through ad-hoc defined threshold ϑ verifying that the level of attention determined by the Drowsiness Monitoring system (through analysis of the PPG signal) is followed according to an φ threshold. The thresholds ϑ and φ are heuristically determined as described in the next sections.

Table 3: Benchmark performance of the proposed pipeline.

	Car Driver Attention Estimation	
	Drowsy Driver	Wakeful Driver
Proposed	98.71 %	99.03 %
(Rundo et al., 2019b)	96.50 %	98.40 %

4 EXPERIMENTAL RESULTS

In this section, we present and analyze the obtained results. To carry out the experiments, we trained and tested the above-described saliency processing system on the DH1FK dataset (Mazzillo et al., 2018), including other driving scenarios acquired by a camera device having a resolution of 2.3 Mpx as and a framerate of 60 fps. Moreover, we trained and tested the 1D-CNN model over several PPG signals sampled on a well recruited dataset. More in detail, under the scientific coordination of physiologists who participated in this study, we recruited several subjects to which we have sampled the PPG signals simulating different attention levels confirmed by the collected EEG signal (Rundo et al., 2019a). Furthermore, we sampled the subject’s PPG signal by using the hardware setup described in this paper with a sampling frequency of 1 kHz. We collected a total of 70 subjects, males and females having an age range from 21 to 70 years. For each recruited subject, the PPG signal was acquired, considering various levels of attention. For each condition (i.e., Drowsy and Wakeful), we collected 5 minutes of PPG signals. Afterward, we subdivided the dataset, consisting of PPG time-series and video driving scenes, taking the 70% of data as the training data and 30% of data as testing and validation data. The table 3 reports the results obtained with the proposed pipeline.

The following Fig. 6 shows some instances of the validated scenarios. In Fig. 6, we show the overall proposed pipeline detecting the required driver’s attention level by analyzing the driving scene us-

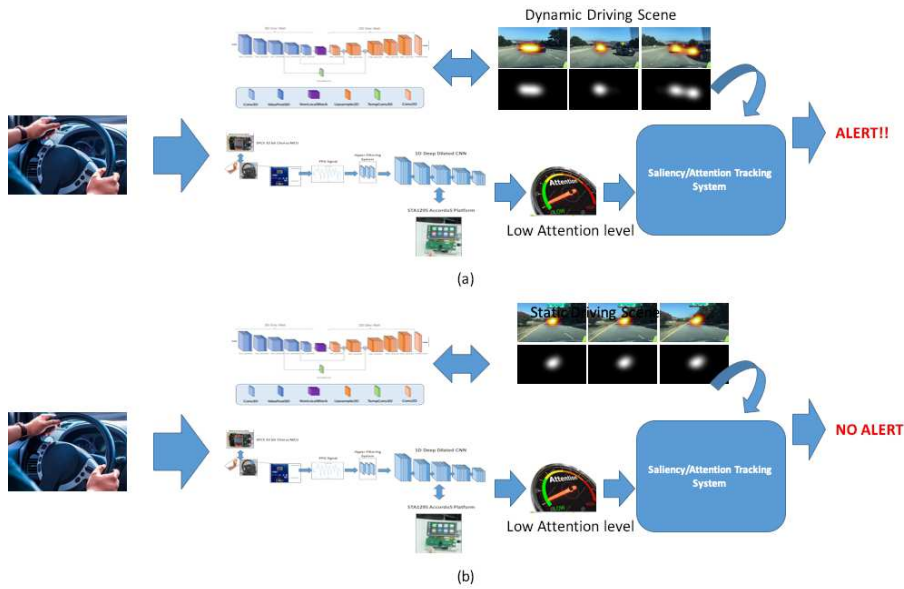


Figure 6: (a) Dynamic driving scenario (car overtaking) requiring high attention level. The Saliency/Attention Tracking System detects an inadequate level of attention generating an acoustic signal alert. (b) Static driving scenario requiring low attention level. The Saliency/Attention Tracking System confirms an adequate level of attention.

ing the NL-FCN pipeline. More specifically, the Saliency/Attention Tracking System compares the level of attention required by the driving scenario with the Drowsiness Monitoring System results. An acoustic signal alerts the driver if the level of attention determined is lower than that required by the driving scenario. For this purpose, we have defined a threshold of $\phi = 0.6$ for the 1D-CNN embedded in the Drowsiness Monitoring System. Specifically, the 1D-CNN output ranges from 0 to 0.6 (threshold) refers to a medium-low attention level, while the range from 0.61 to 1 indicates a high attention level. Consequently, we have defined the ad-hoc normalized ϑ threshold as 0.45 to define a static scene-based saliency map. Therefore, the values of $\frac{\partial S_f(x,y,t)}{\partial t}$ greater than the threshold 0.45, represents a high dynamic driving scene which require high level of the car driver attention. Conversely, saliency maps with low dynamics (under the threshold) will require a low to medium level of attention from the driver.

5 CONCLUSION AND DISCUSSION

This paper introduced an innovative approach that combines visual and physiological data to evaluate the driver’s drowsiness. The obtained results confirmed the robustness of the proposed approach. The main advantage of the method lies in the fact that it does

not require any data analysis in the frequency domain. Furthermore, the proposed method does not require either sampling of the ECG or EEG signals of the driver difficult to be sampled inside the car. The proposed method requires only the PPG signal to be sampled using the described hardware system placed on the steering wheel of the car. Moreover, we evaluated the level of attention by ad-hoc fully convolutional deep network. The proposed network is able to determine a salience map to estimate the attention level for safe driving. Therefore, the proposed pipeline is able to verify whether the level of attention required by the driving scenario is appropriate to the level of attention retrieved by the analysis of the driver’s PPG signal, alerting the driver if a risk mismatch occurs. The proposed pipeline is currently being ported to an embedded system based on the SoC STA1295 ACCORDO 5 MCU platform produced by STMicroelectronics (software environment with embedded Linux) (STMicroelectronics, 2019). To sum up, the results have reported promising results in defining an efficient attention monitoring system. Finally, there are a few directions for further studies. Specifically, we aim to include more robust domain adaptation methods based on the usage of combined supervised and unsupervised approaches successfully used in different applications (Rundo et al., 2019c; Rundo et al., 2019d; Rundo et al., 2018a; Banna et al., 2018).

ACKNOWLEDGEMENTS

The authors thank the physiologists belonging to the Department of Biomedical and Biotechnological Sciences (BIOMETEC) of the University of Catania, who collaborated in this work in the context of the clinical study Ethical Committee CT1 authorization n.113 / 2018 / PO. This research was funded by the National Funded Program 2014-2020 under grant agreement n. 1733, (ADAS + Project). The reported information is covered by the following registered patents: IT Patent Nr. 102017000120714, 24 October 2017. IT Patent Nr. 102019000005868, 16 April 2018; IT Patent Nr. 102019000000133, 07 January 2019.

REFERENCES

- Abi-Saleh, B. and Omar, B. (2019). Einthoven's triangle transparency: a practical method to explain limb lead configuration following single lead misplacements. *Reviews in cardiovascular medicine*, 11(1):33–38.
- Alshaqai, B., Baquhaziel, A. S., Ouis, M. E. A., Boumehed, M., Ouamri, A., and Keche, M. (2013). Driver drowsiness detection system. In *2013 8th International Workshop on Systems, Signal Processing and their Applications (WoSSPA)*, pages 151–155. IEEE.
- Altun, M. and Celenk, M. (2017). Road scene content analysis for driver assistance and autonomous driving. *IEEE transactions on intelligent transportation systems*, 18(12):3398–3407.
- Banna, G. L., Camerini, A., Bronte, G., Anile, G., Addeo, A., Rundo, F., Zanghi, G., Lal, R., and Libra, M. (2018). Oral metronomic vinorelbine in advanced non-small cell lung cancer patients unfit for chemotherapy. *Anticancer research*, 38(6):3689–3697.
- Cai, Y., Liu, Z., Wang, H., and Sun, X. (2017). Saliency-based pedestrian detection in far infrared images. *IEEE Access*, 5:5013–5019.
- Cheon, S.-P. and Kang, S.-J. (2017). Sensor-based driver condition recognition using support vector machine for the detection of driver drowsiness. In *2017 IEEE Intelligent Vehicles Symposium (IV)*, pages 1517–1522. IEEE.
- Choi, H.-T., Back, M.-K., and Lee, K.-C. (2018). Driver drowsiness detection based on multimodal using fusion of visual-feature and bio-signal. In *2018 International Conference on Information and Communication Technology Convergence (ICTC)*, pages 1249–1251. IEEE.
- Deng, T., Yang, K., Li, Y., and Yan, H. (2016). Where does the driver look? top-down-based saliency detection in a traffic driving environment. *IEEE Transactions on Intelligent Transportation Systems*, 17(7):2051–2062.
- Fujiwara, K., Abe, E., Kamata, K., Nakayama, C., Suzuki, Y., Yamakawa, T., Hiraoka, T., Kano, M., Sumi, Y., Masuda, F., et al. (2018). Heart rate variability-based driver drowsiness detection and its validation with eeg. *IEEE Transactions on Biomedical Engineering*, 66(6):1769–1778.
- Hong, T. and Qin, H. (2007). Drivers drowsiness detection in embedded system. In *2007 IEEE International Conference on Vehicular Electronics and Safety*, pages 1–5. IEEE.
- Igasaki, T., Nagasawa, K., Murayama, N., and Hu, Z. (2015). Drowsiness estimation under driving environment by heart rate variability and/or breathing rate variability with logistic regression analysis. In *2015 8th International Conference on Biomedical Engineering and Informatics (BMEI)*, pages 189–193. IEEE.
- Kurian, D., PL, J. J., Radhakrishnan, K., and Balakrishnan, A. A. (2014). Drowsiness detection using photoplethysmography signal. In *2014 Fourth international conference on advances in computing and communications*, pages 73–76. IEEE.
- Mazzillo, M., Maddiona, L., Rundo, F., Sciuto, A., Libertino, S., Lombardo, S., and Fallica, G. (2018). Characterization of sipms with nir long-pass interferential and plastic filters. *IEEE Photonics Journal*, 10(3):1–12.
- Min, K. and Corso, J. J. (2019). Tased-net: Temporally-aggregating spatial encoder-decoder network for video saliency detection. In *Proceedings of the IEEE International Conference on Computer Vision*, pages 2394–2403.
- Rundo, F., Conoci, S., Banna, G. L., Ortis, A., Stanco, F., and Battiato, S. (2018a). Evaluation of levenberg-marquardt neural networks and stacked autoencoders clustering for skin lesion analysis, screening and follow-up. *IET Computer Vision*, 12(7):957–962.
- Rundo, F., Conoci, S., Ortis, A., and Battiato, S. (2018b). An advanced bio-inspired photoplethysmography (ppg) and ecg pattern recognition system for medical assessment. *Sensors*, 18(2):405.
- Rundo, F., Petralia, S., Fallica, G., and Conoci, S. (2018c). A nonlinear pattern recognition pipeline for ppg/ecg medical assessments. In *Convegno Nazionale Sensori*, pages 473–480. Springer.
- Rundo, F., Rinella, S., Massimino, S., Coco, M., Fallica, G., Parenti, R., Conoci, S., and Perciavalle, V. (2019a). An innovative deep learning algorithm for drowsiness detection from eeg signal. *Computation*, 7(1):13.
- Rundo, F., Spampinato, C., and Conoci, S. (2019b). Ad-hoc shallow neural network to learn hyper filtered photoplethysmographic (ppg) signal for efficient car-driver drowsiness monitoring. *Electronics*, 8(8):890.
- Rundo, F., Trenta, F., Di Stallo, A. L., and Battiato, S. (2019c). Advanced markov-based machine learning framework for making adaptive trading system. *Computation*, 7(1):4.
- Rundo, F., Trenta, F., di Stallo, A. L., and Battiato, S. (2019d). Grid trading system robot (gtsbot): A novel mathematical algorithm for trading fx market. *Applied Sciences*, 9(9):1796.

- Ryu, G.-S., You, J., Kostianovskii, V., Lee, E.-B., Kim, Y., Park, C., and Noh, Y.-Y. (2018). Flexible and printed ppg sensors for estimation of drowsiness. *IEEE Transactions on Electron Devices*, 65(7):2997–3004.
- Sari, N. N. and Huang, Y.-P. (2016). A two-stage intelligent model to extract features from ppg for drowsiness detection. In *2016 International Conference on System Science and Engineering (ICSSE)*, pages 1–2. IEEE.
- STMicroelectronics (2019). STMicroelectronics AC-CORDO 5 Automotive Microcontroller. <https://www.st.com/en/automotive-infotainment-and-telematics/automotive-infotainment-socs.html?icmp=tt4379-gl-pron-nov2016>. (accessed on 02 July 2019).
- Szypulska, M. and Piotrowski, Z. (2012). Prediction of fatigue and sleep onset using hrv analysis. In *Proceedings of the 19th International Conference Mixed Design of Integrated Circuits and Systems-MIXDES 2012*, pages 543–546. IEEE.
- Vicente, J., Laguna, P., Bartra, A., and Bailón, R. (2011). Detection of driver's drowsiness by means of hrv analysis. In *2011 Computing in Cardiology*, pages 89–92. IEEE.
- Vinciguerra, V., Ambra, E., Maddiona, L., Romeo, M., Mazzillo, M., Rundo, F., Fallica, G., di Pompeo, F., Chiarelli, A. M., Zappasodi, F., et al. (2018). Ppg/ecg multisite combo system based on sipm technology. In *Convegno Nazionale Sensori*, pages 353–360. Springer.
- Wang, X., Girshick, R., Gupta, A., and He, K. (2018). Non-local neural networks. In *Proceedings of the IEEE conference on computer vision and pattern recognition*, pages 7794–7803.
- Winterlich, A., Zlokolica, V., Denny, P., Kilmartin, L., Glavin, M., and Jones, E. (2013). A saliency weighted no-reference perceptual blur metric for the automotive environment. In *2013 Fifth International Workshop on Quality of Multimedia Experience (QoMEX)*, pages 206–211. IEEE.
- Xu, Y. J., Ding, F., Wu, Z., Wang, J., Ma, Q., Chon, K., Clancy, E., Qin, M., Mendelson, Y., Fu, N., et al. (2012). Drowsiness control center by photoplethysmogram. In *2012 38th Annual Northeast Bioengineering Conference (NEBEC)*, pages 430–431. IEEE.